

Detection of DEfects and HYDROgen by ion beam analysis in Channeling mode for fusion – DeHydroC

Project code: ENR-MAT-01-JSI

Monitoring meeting - activities 2022
7. February 2023

Sabina Markelj (PI) on behalf of the team



MAX-PLANCK-INSTITUT
FÜR PLASMAPHYSIK



Team members



MAX-PLANCK-INSTITUT
FÜR PLASMAPHYSIK

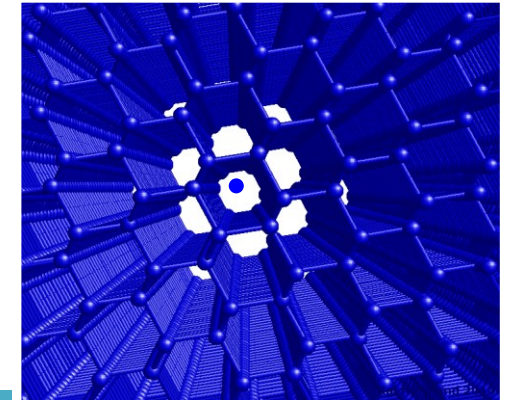
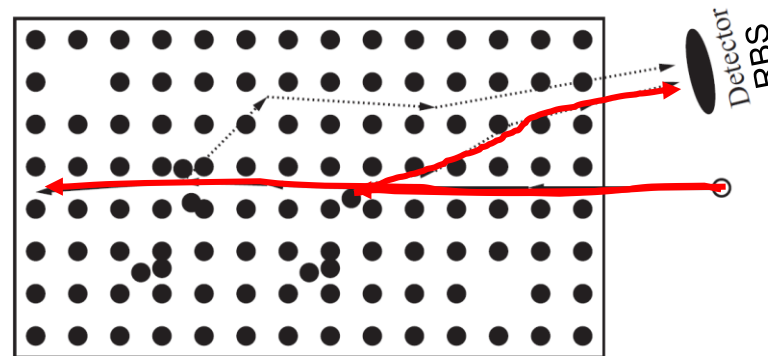


Beneficiary	Names	Expertise	Contact
JSI	Sabina Markelj	HI interaction, sample irradiation, ion beam analysis (IBA)	sabina.markelj@ijs.si
	Esther Punzón Quijorna	Channelling, IBA (Post-doc)	esther.punzon-quiorna@ijs.si
	Mitja Kelemen	Construction, IBA, channelling (PhD, Post-doc)	mitja.kelemen@ijs.si
	Matjaž Vencelj	Detectors	matjaz.vencelj@ijs.si
	Primož Pelicon	IBA, construction, channelling	Primož.Pelicon@ijs.si
	Janez Zavašnik	TEM/SEM	janez.zavasnik@ijs.si
	Andreja Šestan	TEM/SEM, sample preparation (PhD, Post-doc)	andreja.sestan@ijs.si
	MPG	Thomas Schwarz-Selinger	Sample irradiation, IBA, HI interaction, TDS
Wolfgang Jacob		HI interaction, TDS	Wolfgang.Jacob@ipp.mpg.de
UHEL	Flyura Djurabekova	Multiscale modelling, RBSADEC development	flyura.djurabekova@helsinki.fi
	Xin Jin	Code development, MD, RBSADEC (PhD)	xin.jin@helsinki.fi
	Ilja Makkonen	DFT for RBSADEC (Post-doc)	Ilja.makkonen@helsinki.fi
	Tommy Ahlgren	IBA, HI interaction, MRE modelling	tommy.ahlgren@helsinki.fi
	Kenichiro Mizohata	IBA, RBS-channelling	kenichiro.mizohata@helsinki.fi
	Filip Tuomisto	PAS	filip.tuomisto@helsinki.fi
CEA	Christian Grisolia	MRE modelling	Christian.GRISOLIA@cea.fr
	Etienne Hodille	MRE modelling, MD	Etienne.HODILLE@cea.fr

RBS channeling



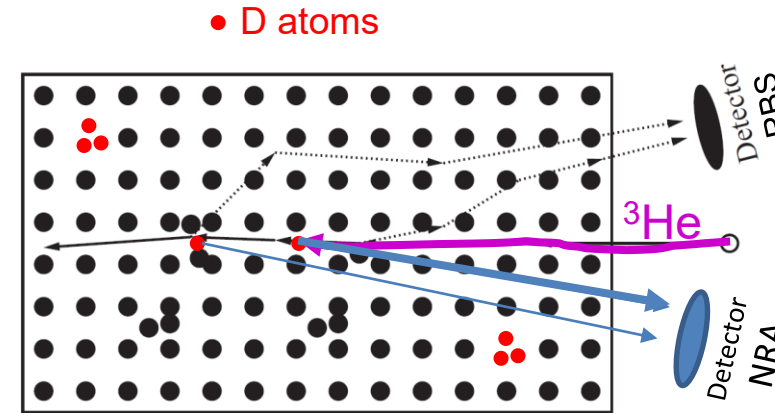
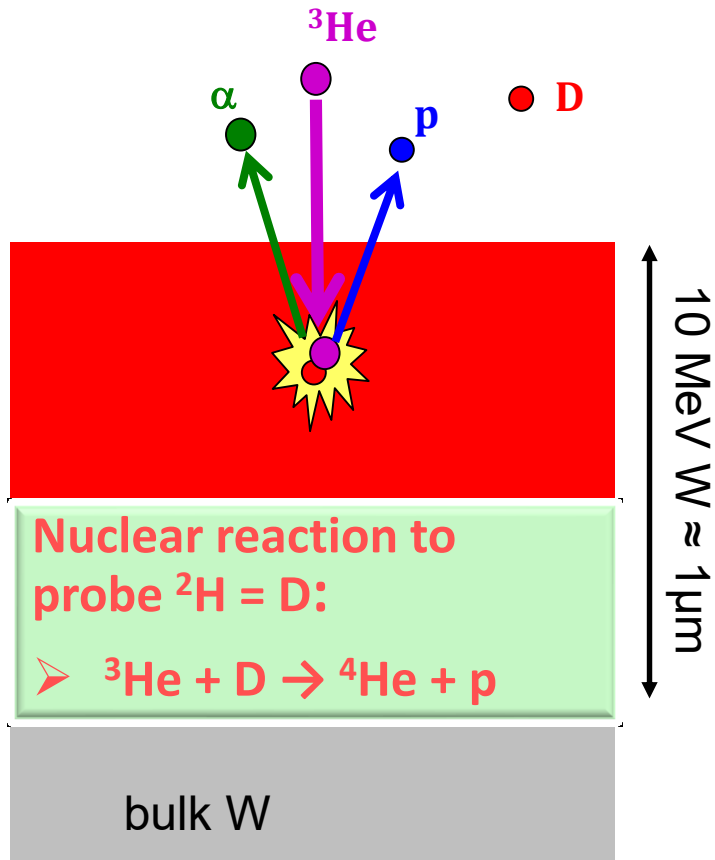
Channeling Rutherford Backscattering Spectroscopy (C-RBS) is a well known method to measure disorder in materials due to ion irradiation



- Objective 1: Identify defects in displacement-damaged tungsten by C-RBS with help of microstructure analysis methods by:
 - Electron Microscopy (SEM, TEM, STEM,
 - Positron Spectroscopy (PALS, DB-PAS)

Sensitive mainly to dislocation structure (loops, lines)

D retention analysis by nuclear reaction analysis (NRA)



- Objective 2: perform NRA in channelling mode on a quantitative level to allow for determination of absolute deuterium amounts inside individual defects.

Deuterium trapped in open volume (vacancies, vacancy clusters, voids)

- C-RBS and C-NRA complementary for defect characterization

Deuterium depth profiles - Analyzing protons from nuclear reaction $\text{D}(^3\text{He},p)^4\text{He}$ at different ^3He energies from 700 keV up to 4.3 MeV



- Task 1.1 Incorporation of the goniometer in the INSIBA experimental station – JSI.
 - D2.1 (Task 1.1) Commissioning of the goniometer with cooling and heating capabilities. (M1)
- Task 1.2 Detection system for ion beam methods
 - D2.2 (Task 1.2) Purchase of the PSD and acquisition system. (M2)
- Task 2.1 Production of samples with dominant defects in the material – MPG and JSI.
 - Second batch with well-defined displacement damage.
- Task 2.2 Characterization of defects –UHEL, JSI, MPG.
 - D2.3 (Task 2.2) Microstructure data on samples with dominant defect type, first C-RBS spectra. (M4)
- Task 2.3 Simulation and interpretation of C-RBS spectra - UHEL, CEA, JSI.
 - D2.4 (Task 2.3) Incorporation of defect structures into RBSADEC. (M5)
- Task 3.1 Characterization of defects by D retention studies and MRE modelling - JSI, MPG, CEA, UHEL.
 - D2.5 (Task 3.1) Determine the de-trapping energies of D in defects and correlate with the defect characterization techniques. (M7)
- Task 3.3 – Modelling of deuterium position in lattice/defect and identification of D position - UHEL, CEA, JSI.
 - D2.6 (Task 3.3) DFT calculations for D positions in defects, code development for C-NRA.



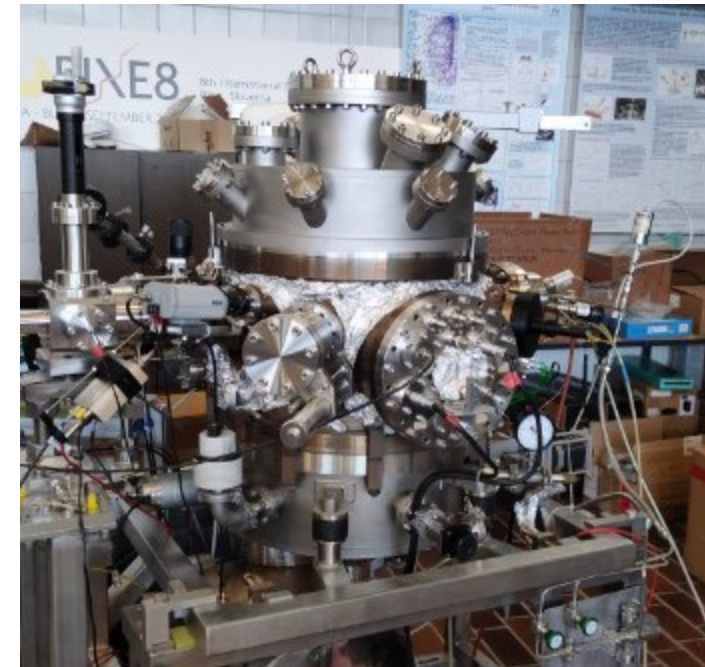
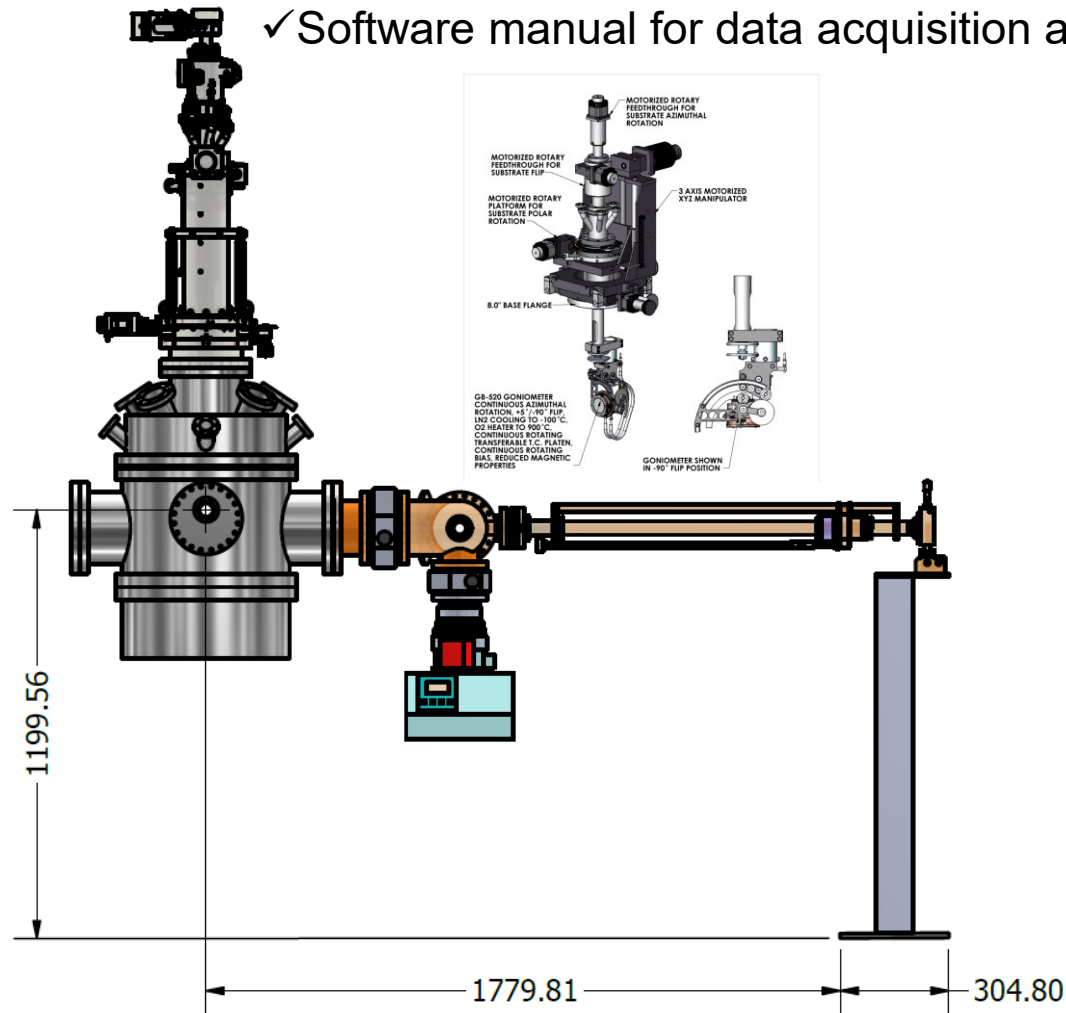
- **Task 1.1 Incorporation of the goniometer in the INSIBA experimental station – JSI.**
 - D2.1 (Task 1.1) Commissioning of the goniometer with cooling and heating capabilities. (M1)
- **Task 1.2 Detection system for ion beam methods**
 - D2.2 (Task 1.2) Purchase of the PSD and acquisition system. (M2)
- **Task 2.1 Production of samples with dominant defects in the material – MPG and JSI.**
 - Second batch with well-defined displacement damage.
- **Task 2.2 Characterization of defects –UHEL, JSI, MPG.**
 - D2.3 (Task 2.2) Microstructure data on samples with dominant defect type, first C-RBS spectra. (M4)
- **Task 2.3 Simulation and interpretation of C-RBS spectra - UHEL, CEA, JSI.**
 - D2.4 (Task 2.3) Incorporation of defect structures into RBSADEC. (M5)
- **Task 3.1 Characterization of defects by D retention studies and MRE modelling - JSI, MPG, CEA, UHEL.**
 - D2.5 (Task 3.1) Determine the de-trapping energies of D in defects and correlate with the defect characterization techniques. (M7)
- **Task 3.3 – Modelling of deuterium position in lattice/defect and identification of D position - UHEL, CEA, JSI.**
 - D2.6 (Task 3.3) DFT calculations for D positions in defects, code development for C-NRA.

6-axis goniometer



- ✓ JSI – 6-axis goniometer specified, public call, final order at National Electrostatic Corp. (NEC) 08/2021 (Delays due to Covid-19 and Ukraine war): Partial delivery in October 2022 – full delivery promised for February 2023 but now postponed further - serious issue for 2023?

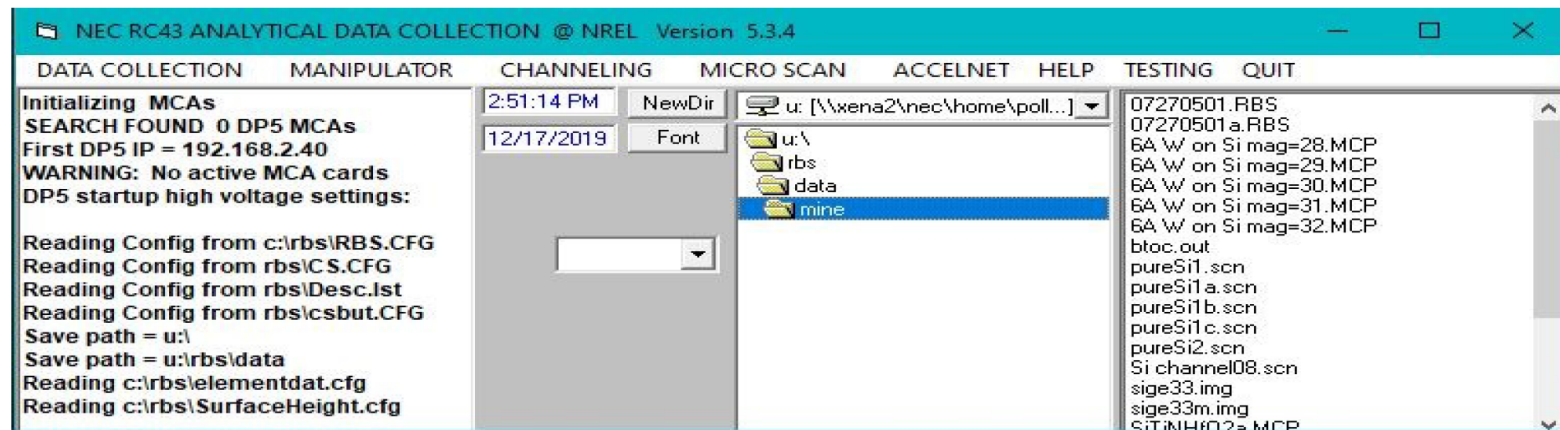
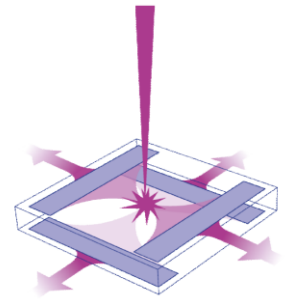
- ✓ Software manual for data acquisition and goniometer



New cover for the vacuum chamber – mounted on the chamber



- Position sensitive detector delivered by SiTeC electro optics – acquisition system being produced in house:
- Other options to increase the detection efficiency – decrease analyzing time
 - Purchase large square NRA detector to cover larger solid angle
 - Have two NRA detectors each on one side at the same angle
- Detection system (without the detectors) and computer control for data acquisition and manipulator come with the goniometer





- Task 1.1 Incorporation of the goniometer in the INSIBA experimental station – JSI.
 - D2.1 (Task 1.1) Commissioning of the goniometer with cooling and heating capabilities. (M1)
- Task 1.2 Detection system for ion beam methods
 - D2.2 (Task 1.2) Purchase of the PSD and acquisition system. (M2)
- Task 2.1 Production of samples with dominant defects in the material – MPG and JSI.
 - Second batch with well-defined displacement damage.
- Task 2.2 Characterization of defects –UHEL, JSI, MPG.
 - D2.3 (Task 2.2) Microstructure data on samples with dominant defect type, first C-RBS spectra. (M4)
- Task 2.3 Simulation and interpretation of C-RBS spectra - UHEL, CEA, JSI.
 - D2.4 (Task 2.3) Incorporation of defect structures into RBSADEC. (M5)
- Task 3.1 Characterization of defects by D retention studies and MRE modelling - JSI, MPG, CEA, UHEL.
 - D2.5 (Task 3.1) Determine the de-trapping energies of D in defects and correlate with the defect characterization techniques. (M7)
- Task 3.3 – Modelling of deuterium position in lattice/defect and identification of D position - UHEL, CEA, JSI.
 - D2.6 (Task 3.3) DFT calculations for D positions in defects, code development for C-NRA.

Tungsten single crystals (111) - Samples prepared



Decided to go with only 10.8 MeV W ion irradiation, according to recent publications [Hu et al. JNM 556 (2021) 153175]

- Mainly single vacancies at room temperature
- Larger vacancy clusters at 773 K

Expectations based on:

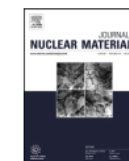
Journal of Nuclear Materials 556 (2021) 153175



Contents lists available at ScienceDirect

Journal of Nuclear Materials

journal homepage: www.elsevier.com/locate/jnucmat



✓ For PAS/PALS analysis Helsinki (2022)

	ID	Definition
1)	78a	'Heavily damaged standard': 0.2dpa, 290K
2)	78h	'Single vacancies': 0.02 dpa, 290 K
3)	78e	'Big vacancy clusters': 0.2 dpa, 800 K
4)	78d	'Small vacancy clusters': 0.02 dpa, 800 K

Effect of purity on the vacancy defects induced in self-irradiated tungsten: A combination of PAS and TEM

Z. Hu^a, P. Desgardin^a, C. Genevois^a, J. Joseph^a, B. Décamps^b, R. Schäublin^c, M-F. Barthe^{a,*}

^a CEMHTI, CNRS, UPR3079, University of Orléans, F-45071 Orléans, France

^b JJCLab/CNRS, Paris - Saclay University, France

^c Laboratory of Metal Physics and Technology, Department of Materials, ETH Zurich, Switzerland





Lifetimes for non-irradiated samples

Samples	Positron lifetime (ps)
78a+78e	116
78d+78e	118
1700W+78a	110
78a+78d	108

The average positron lifetime in the non-irradiated sample has been determined as 108 ps;

- **Excellent crystalline quality**

Lifetimes for irradiated samples

Samples	Damage dose (dpa)	Irradiation temperature
78a	0.2	RT
78h	0.02	RT
78d	0.02	800 K
78e	0.2	800 K

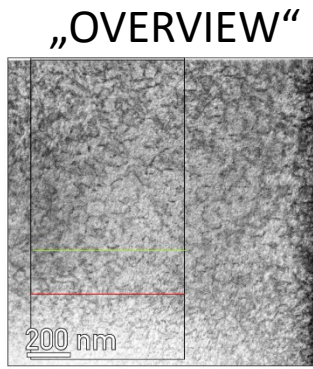
Samples	Positron average lifetime (ps)
78a+78h (RT)	~ 138 ps
78d+78e (800 K)	~ 200 ps

- Average positron lifetime **increased with irradiation**
- Shorter lifetime – smaller defects (vacancies)
- Depth profiling planned for February 2023

TEM analysis

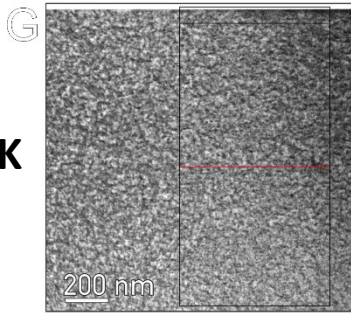
Summary page

78f 0.2 dpa 290 K



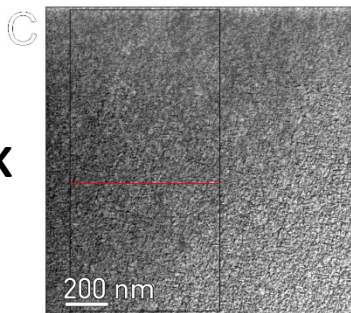
depth:
(0.9)-1.1 μm

78g 0.02 dpa 290 K



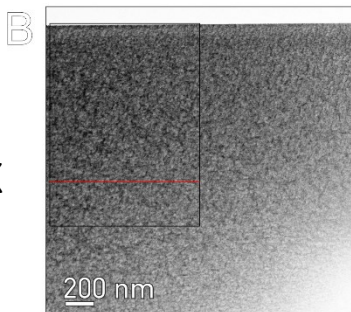
depth:
0.7 μm

78c 0.02 dpa 800 K



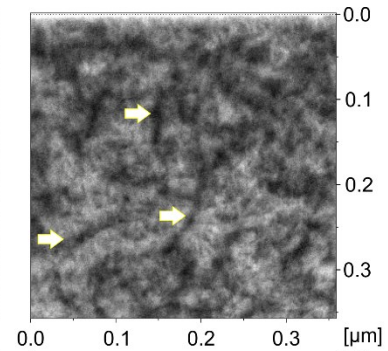
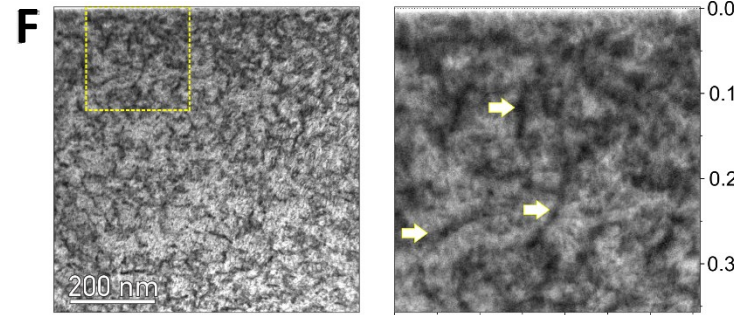
depth:
0.8 μm

78b 0.2 dpa 800 K

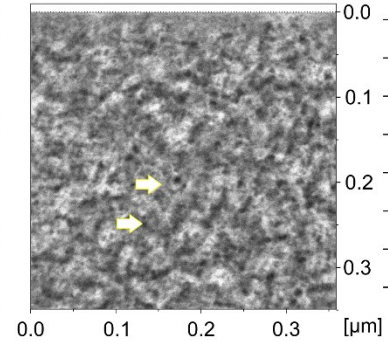
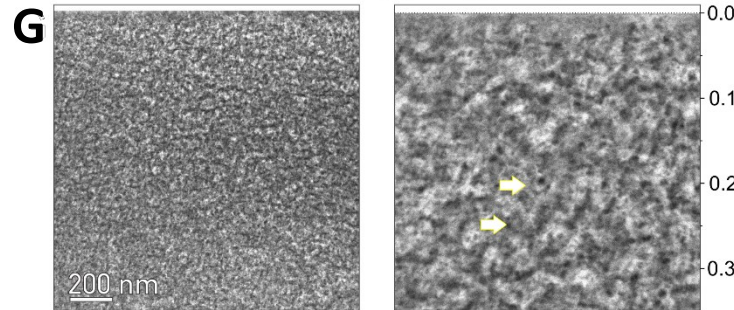


depth:
 $\sim 1.1 - 1.2 \mu\text{m}$

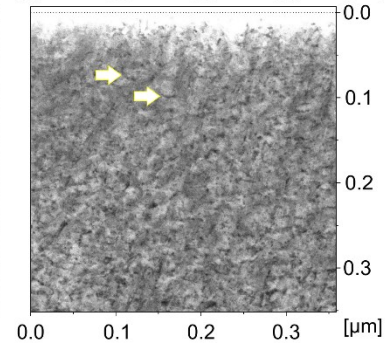
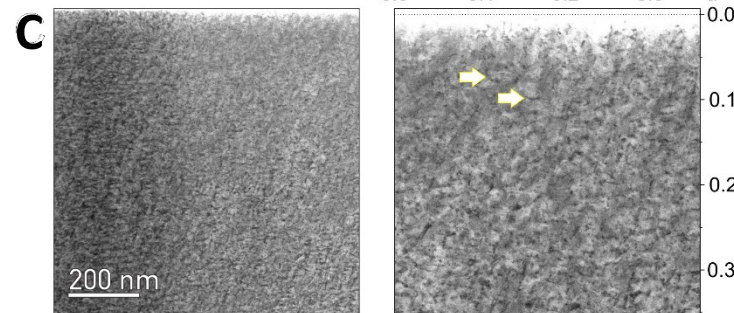
„ZOOM IN“



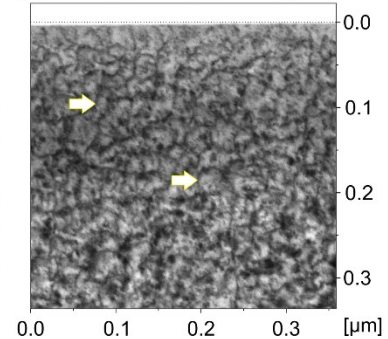
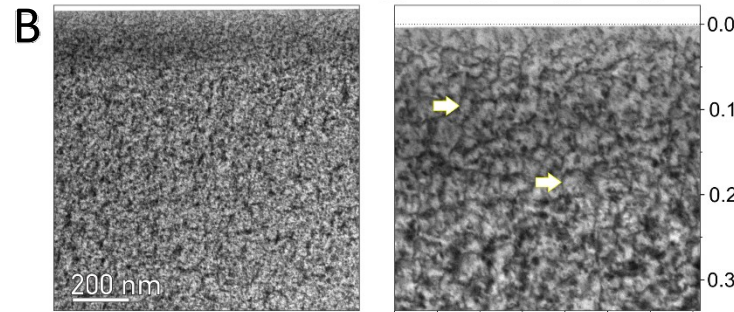
Dense network of dislocation lines ($\sim 100+$ nm), which are already nicely visible at low-mag overview micrographs. Directions of DL lines coincide with $110 > 111 > 11\text{-}2 > 111$ planes.



Only very short dislocation lines ($\sim 20\text{-}30$ nm) in $\langle 111 \rangle$, with prevailing U-shaped loops around “black dots” (size ~ 10 nm)



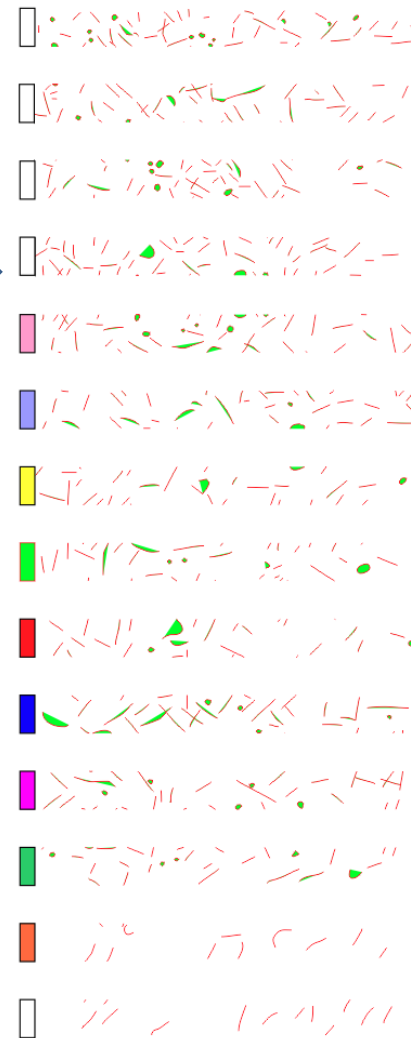
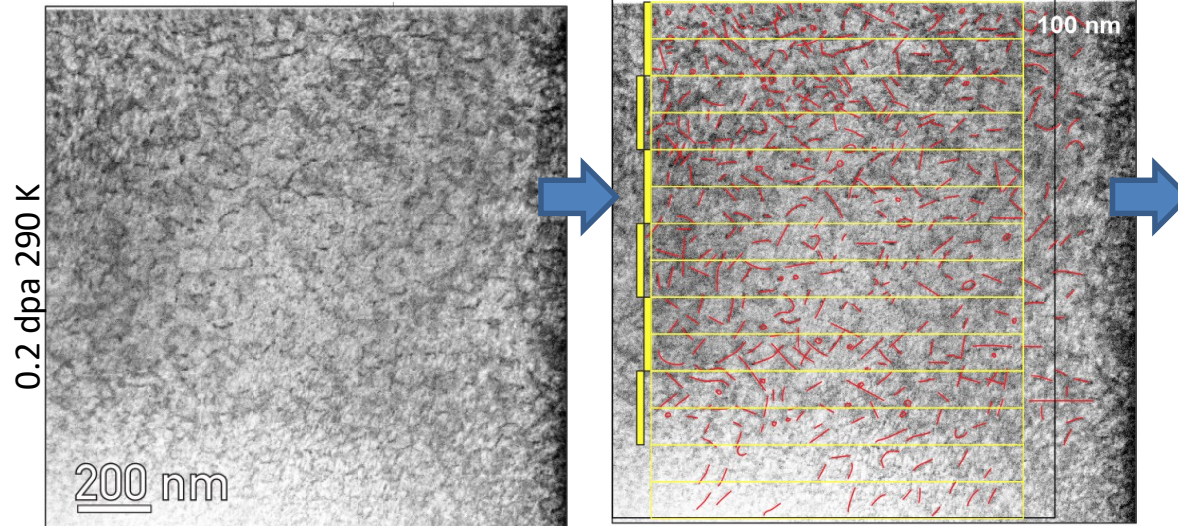
Dislocations: mainly dots and several isolated lines (< 50 nm, in $\langle 111 \rangle$ direction). Dots are smaller, several nm.



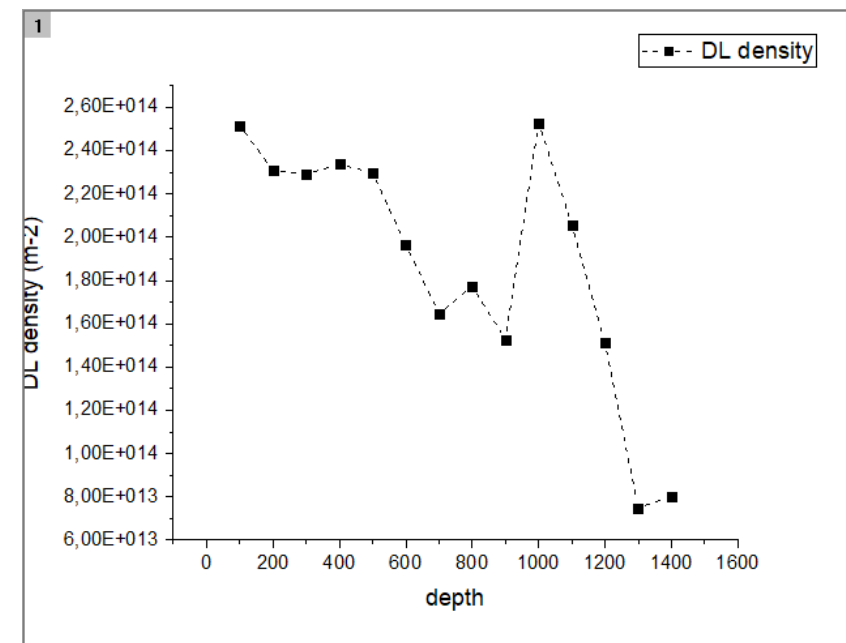
Several dislocation lines and larger black dots. DL lines are forming a network in $\langle 111 \rangle$, forming square “polygons” with ~ 30 nm edge.

TEM analysis of SC W (111) – sample 0.2 dpa 300 K

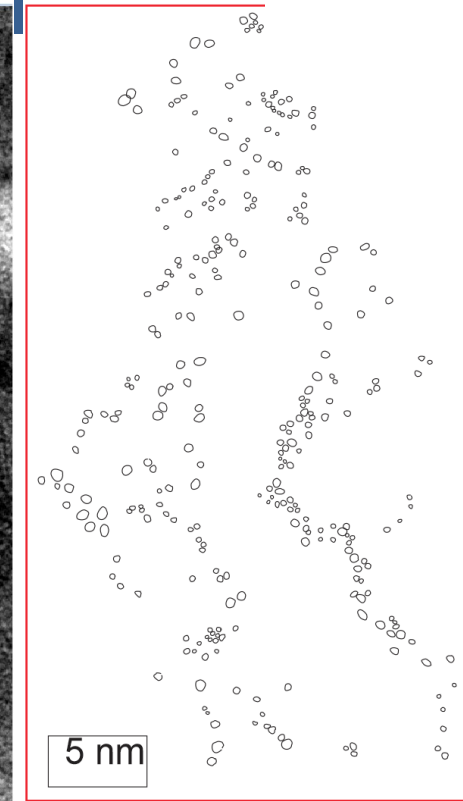
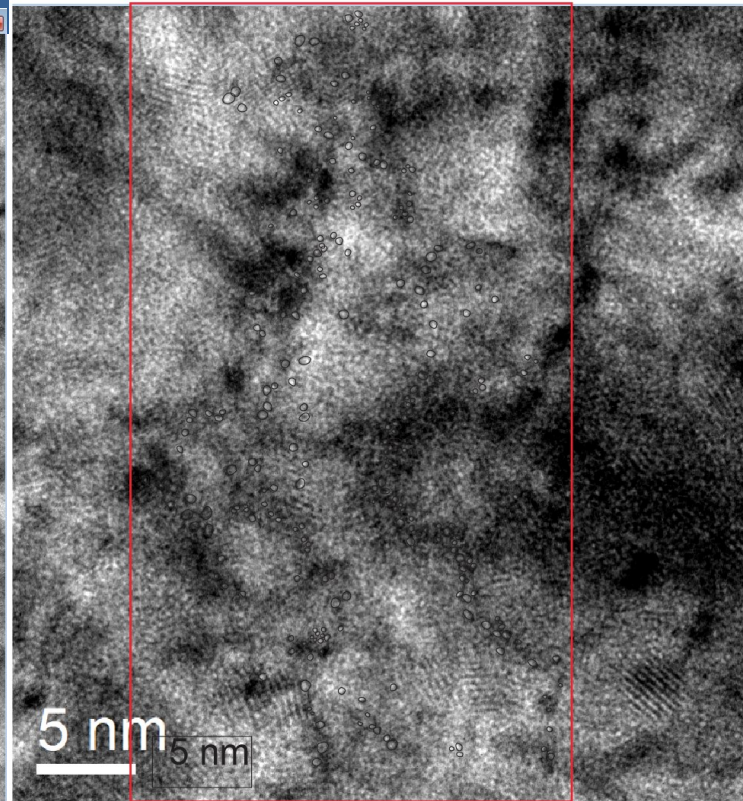
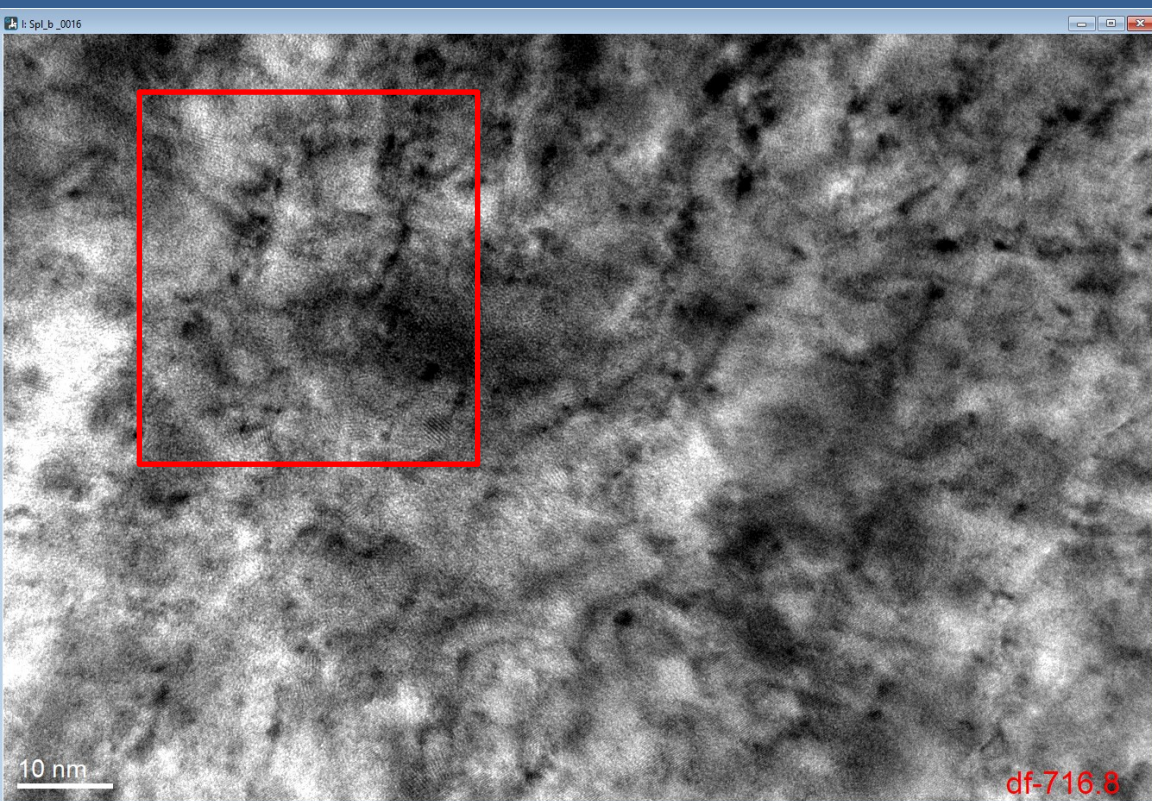
Average dislocation line density: $1.88 \cdot 10^{14} \text{ m/m}^3$



RANGE	No. of DLs	total length [nm]:	density
1. 000-100 nm	N = 56	length: 1760.8	$2.52 \cdot 10^{14}$
2. 100-200 nm	N = 52	length: 1615.9	$2.31 \cdot 10^{14}$
3. 200-300 nm	N = 51	length: 1604.0	$2.29 \cdot 10^{14}$
4. 300-400 nm	N = 53	length: 1636.1	$2.34 \cdot 10^{14}$
5. 400-500 nm	N = 46	length: 1608.0	$2.30 \cdot 10^{14}$
6. 500-600 nm	N = 40	length: 1376.0	$1.97 \cdot 10^{14}$
7. 600-700 nm	N = 38	length: 1152.7	$1.65 \cdot 10^{14}$
8. 700-800 nm	N = 40	length: 1240.8	$1.77 \cdot 10^{14}$
9. 800-900 nm	N = 29	length: 1069.3	$1.53 \cdot 10^{14}$
10. 900-1000 nm	N = 38	length: 1769.9	$2.53 \cdot 10^{14}$
11. 1000-1100 nm	N = 34	length: 1440.3	$2.06 \cdot 10^{14}$
12. 1100-1200 nm	N = 31	length: 1057.1	$1.51 \cdot 10^{14}$
13. 1200-1300 nm	N = 12	length: 524.4	$7.49 \cdot 10^{13}$
14. 1300-1400 nm	N = 10	length: 562.7	$8.04 \cdot 10^{13}$



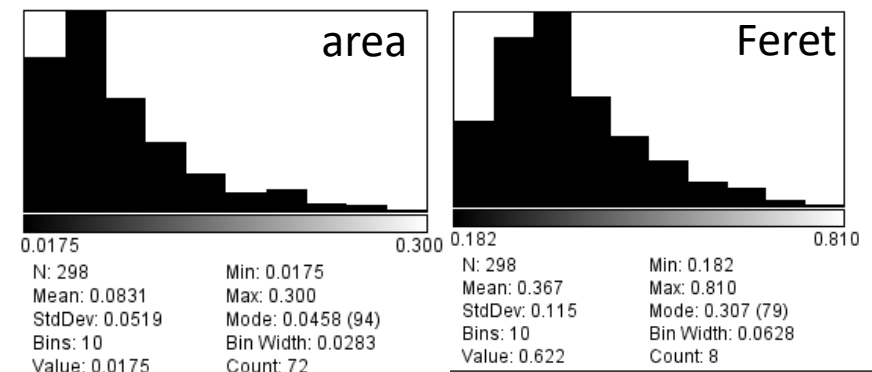
TEM analysis of sample "78b", 0.2 dpa 800 K (voids?)



➤ **mean diameter of 0.37 nm**
(resolution $\approx 1.2 \text{ \AA} \Rightarrow 0.12 \text{ nm}$)

➤ **void density $5 \times 10^{24} \text{ m}^{-3}$**

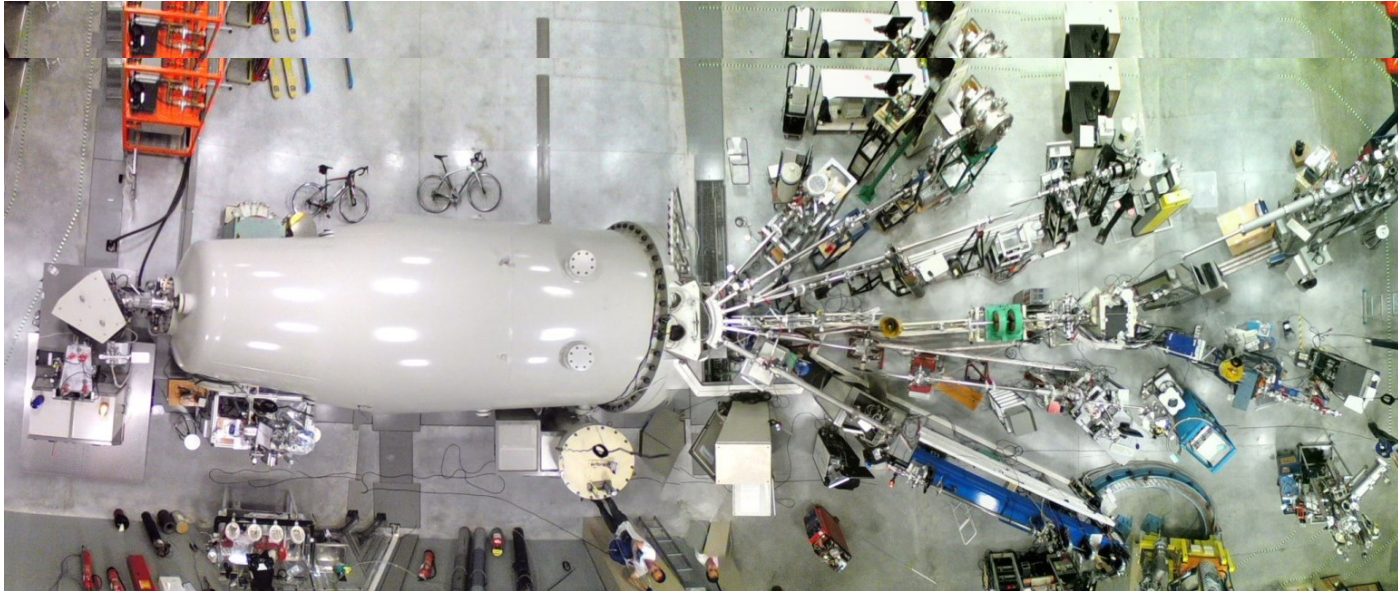
(only rough estimation from 1 example & limited area!)



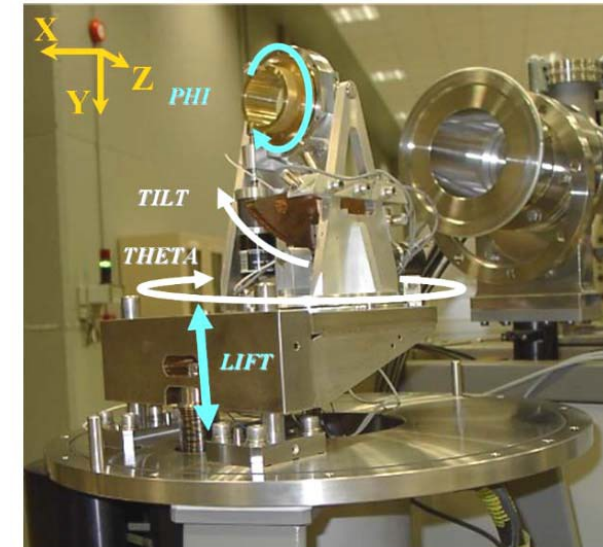
Analysis of irradiated samples by C-RBS in Madrid



- **Second visit** of JSI team to *CMAM (Centre for Micro Analysis of Materials), UAM (Madrid.)* for C-RBS measurements in **October 2022**



5MV Accelerator Cockcroft-Walton (High Voltage Europe)



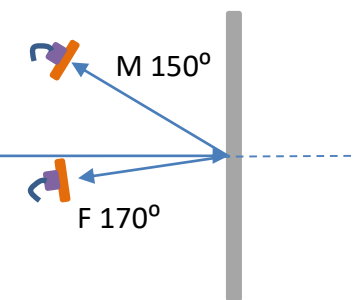
3 angles goniometer
(no heating)
(Panmure Instruments, UK)

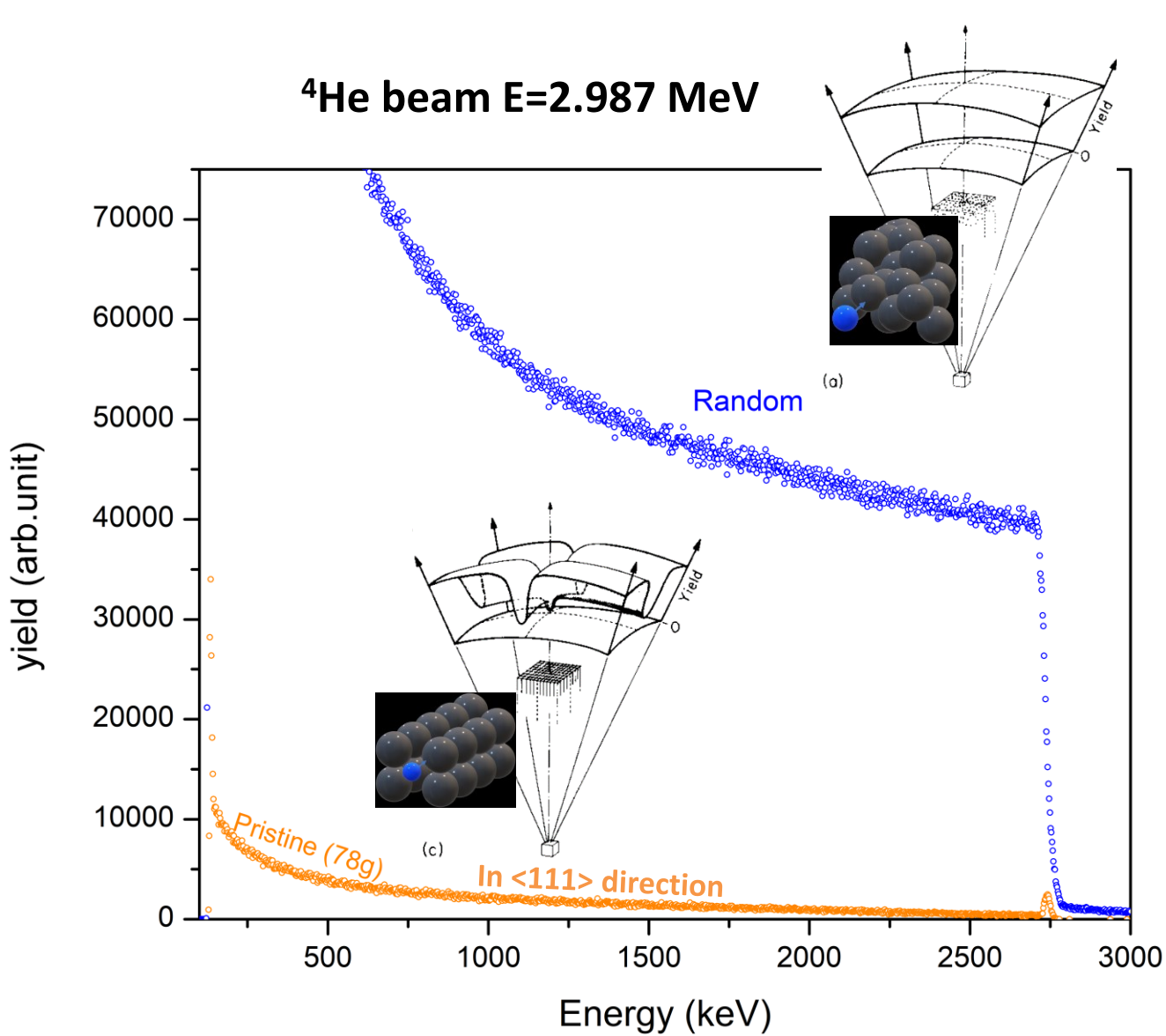
With the goal to differentiate defect structures in the channelling-RBS spectra: **we have performed a multi-energy axial channeling study in order to obtain additional information about the nature of the defects.**

Set up

^4He Beam $E=2,987$ MeV

$E= 3, 3.5, 4, 4.5$ MeV





Random = $\Sigma 100$ spectra (5 μC) – nonchanneling

$\langle 111 \rangle$ channelling direction

78f heavily damaged standard: 0.2 dpa 290 K

78g single vacancies: 0.02 dpa 290 K

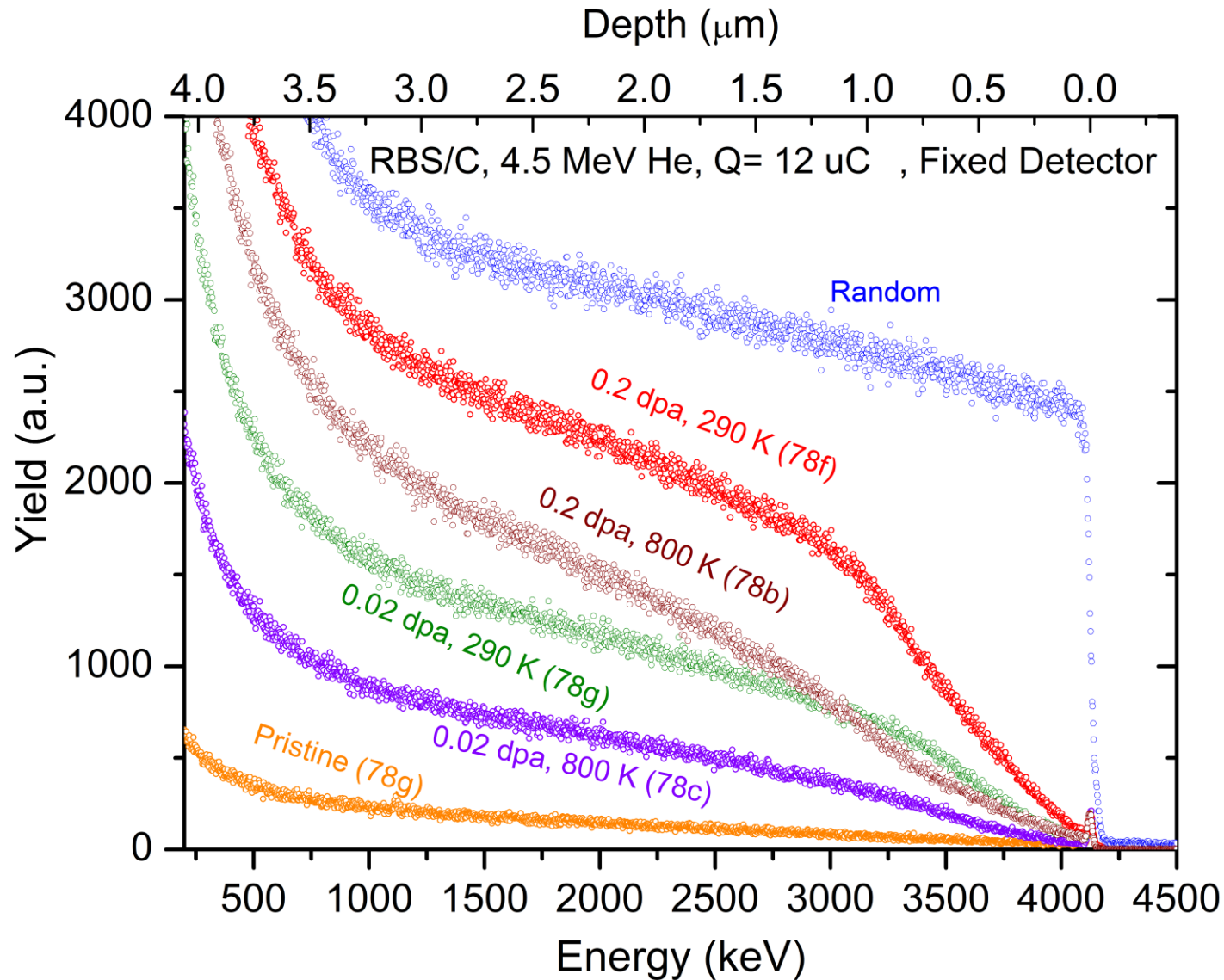
78c small vacancy clusters: 0.02 dpa 800 K

78b big vacancy clusters: 0.2 dpa 800 K

78g pristine

✓ Starting material (pristine sample) has a very good crystallinity

Energy spectra @ 4.5 MeV



Random = Σ 100 spectra – nonchanneling

<111> channelling direction

78f heavily damaged standard: 0.2 dpa 290 K

78g single vacancies: 0.02 dpa 290 K

78c small vacancy clusters: 0.02 dpa 800 K

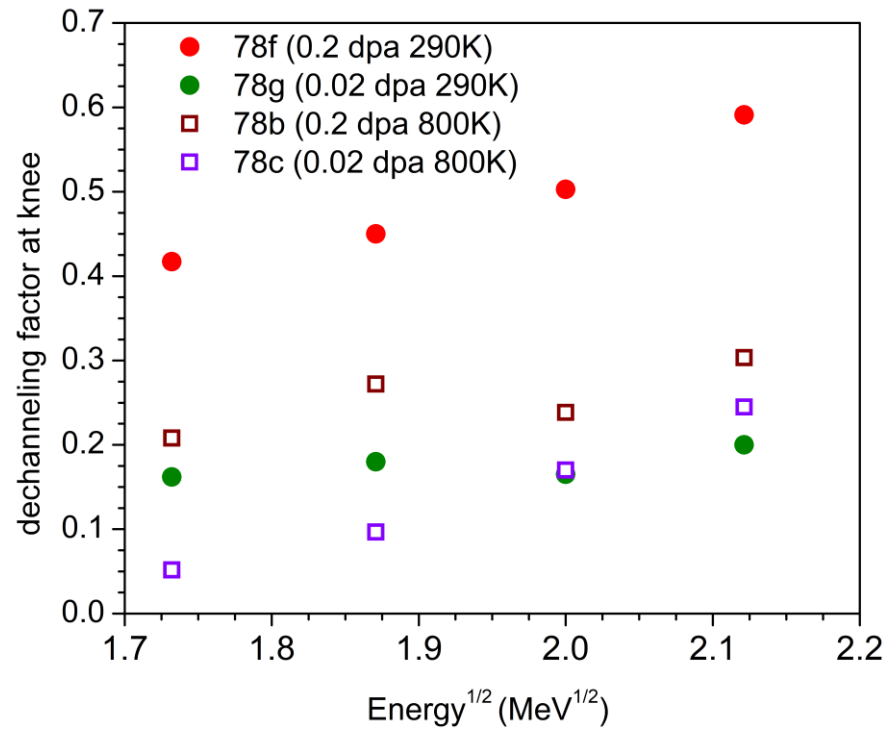
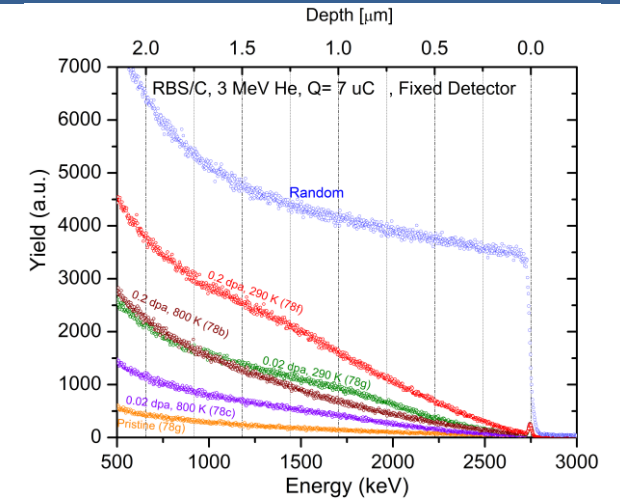
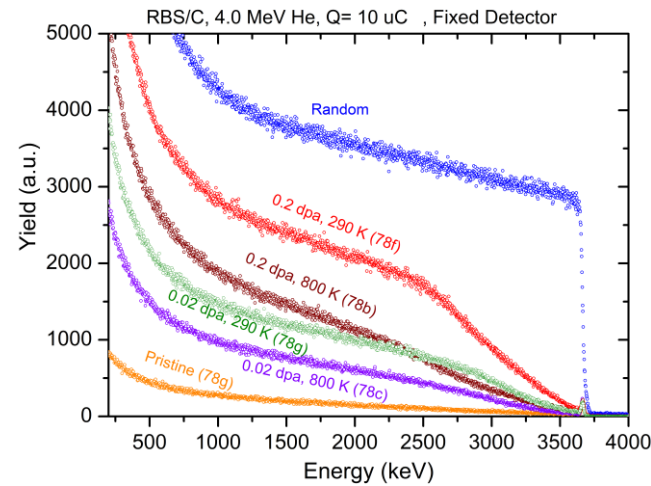
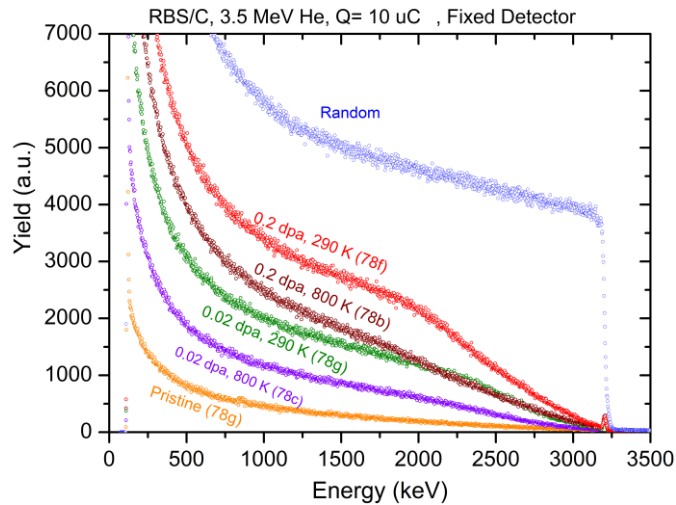
78b big vacancy clusters: 0.2 dpa 800 K

78g pristine

Ratio of the signal between Pristine/Random after the surface peak = 1.3 %

- **Excellent crystallinity of the sample**
- **We have observed differences between the irradiation damage treatments**

Energy spectra @ other energies



Dechanneling factor as a function of energy

- 78f – positive slope – extended defects – dislocation lines (TEM)
- 78g – no slope – discontinuous defects – small dislocation loops (TEM)
- 78b – no slope
- 78c – positive slope
- Following: *FELDMAN, MATERIALS ANALYSIS BY ION CHANNELING. Submicron Crystallography, 1982, Academic press*

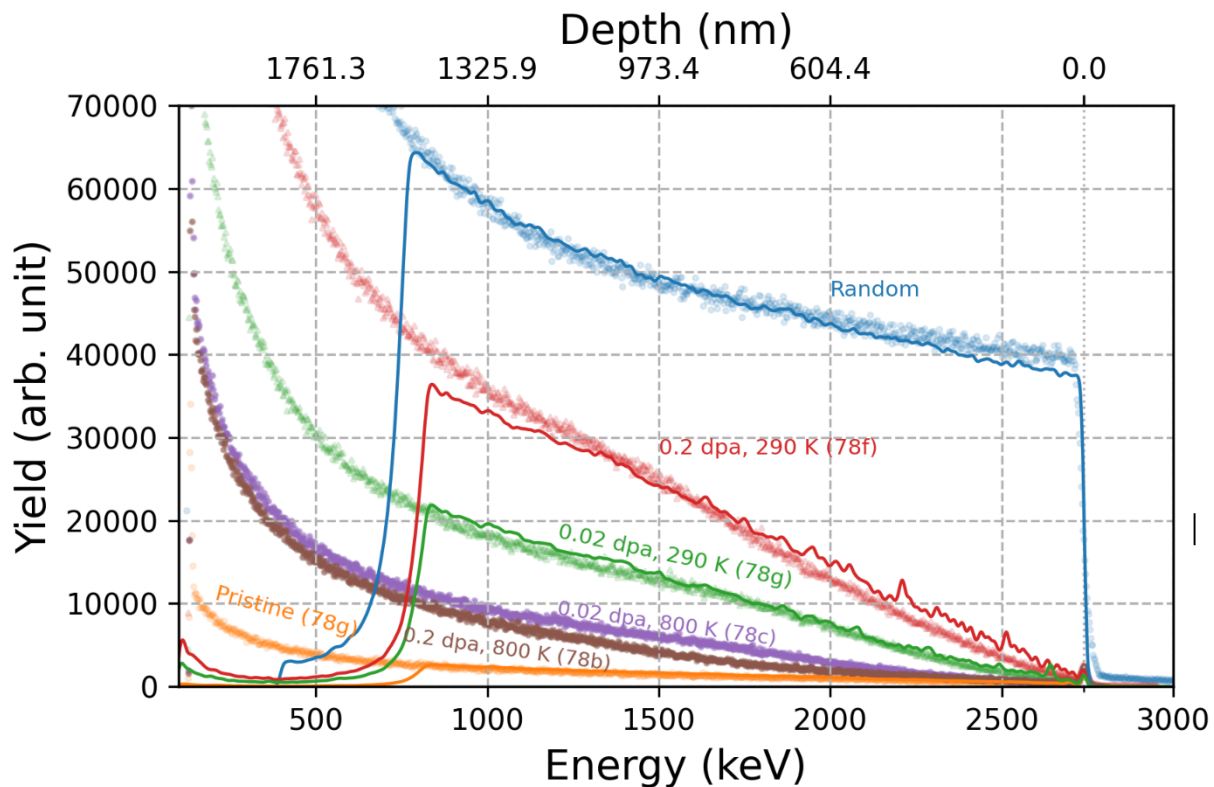
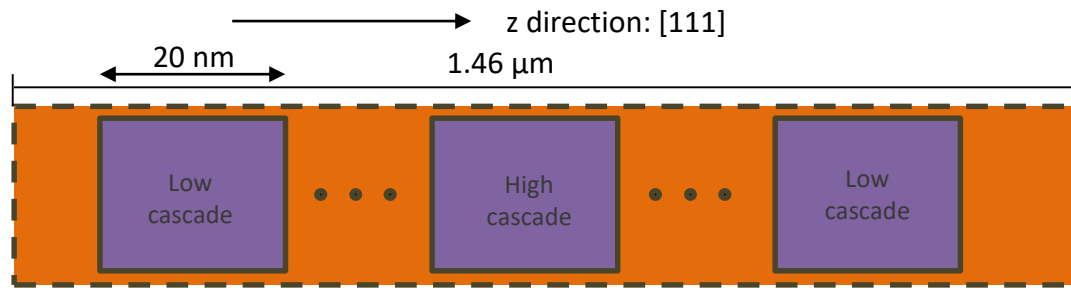


- Task 1.1 Incorporation of the goniometer in the INSIBA experimental station – JSI.
 - D2.1 (Task 1.1) Commissioning of the goniometer with cooling and heating capabilities. (M1)
- Task 1.2 Detection system for ion beam methods
 - D2.2 (Task 1.2) Purchase of the PSD and acquisition system. (M2)
- Task 2.1 Production of samples with dominant defects in the material – MPG and JSI.
 - Second batch with well-defined displacement damage.
- Task 2.2 Characterization of defects –UHEL, JSI, MPG.
 - D2.3 (Task 2.2) Microstructure data on samples with dominant defect type, first C-RBS spectra. (M4)
- Task 2.3 Simulation and interpretation of C-RBS spectra - UHEL, CEA, JSI.
 - D2.4 (Task 2.3) Incorporation of defect structures into RBSADEC. (M5)
- Task 3.1 Characterization of defects by D retention studies and MRE modelling - JSI, MPG, CEA, UHEL.
 - D2.5 (Task 3.1) Determine the de-trapping energies of D in defects and correlate with the defect characterization techniques. (M7)
- Task 3.3 – Modelling of deuterium position in lattice/defect and identification of D position - UHEL, CEA, JSI.
 - D2.6 (Task 3.3) DFT calculations for D positions in defects, code development for C-NRA.

Calculations and fits of C-RBS spectra by RBSADEC simulation using Molecular Dynamics cells



➤ Take real defect structures from MD



➤ Generation of defects in MD cells

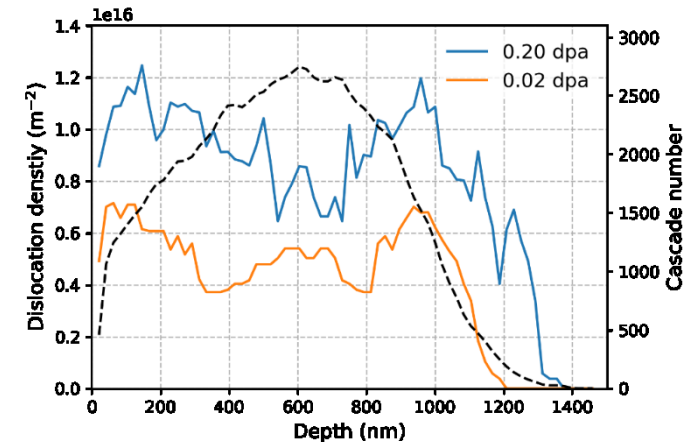
☐ 10 keV cascades

☐ Number of collision cascade ↔ displacement damage dose (NRT)

☐ Connection of W MD cells:

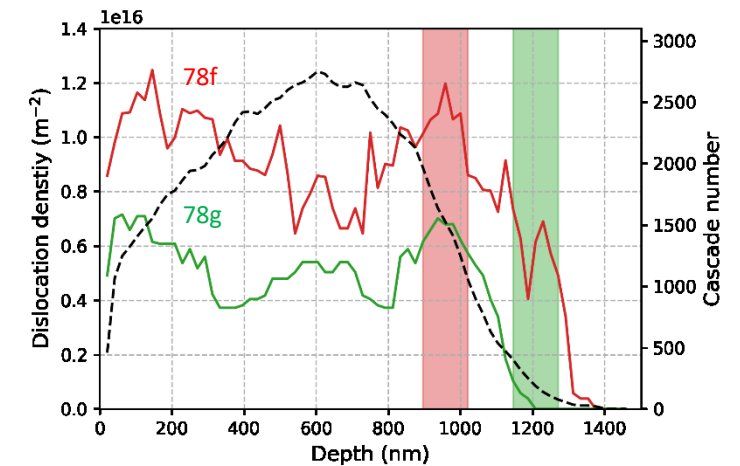
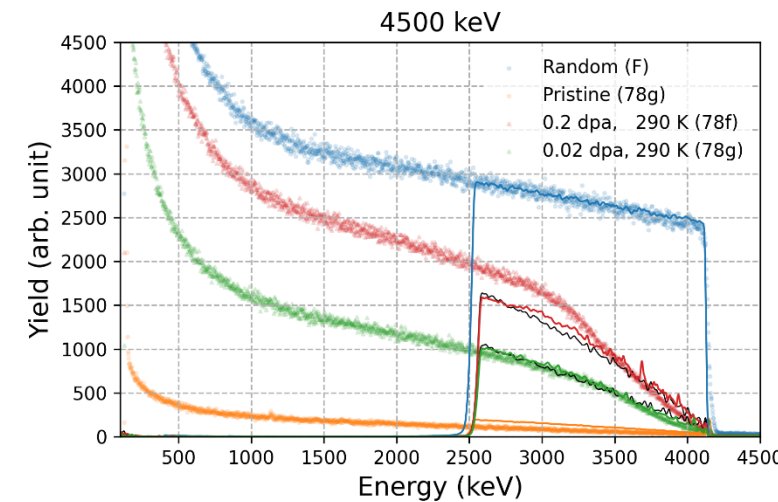
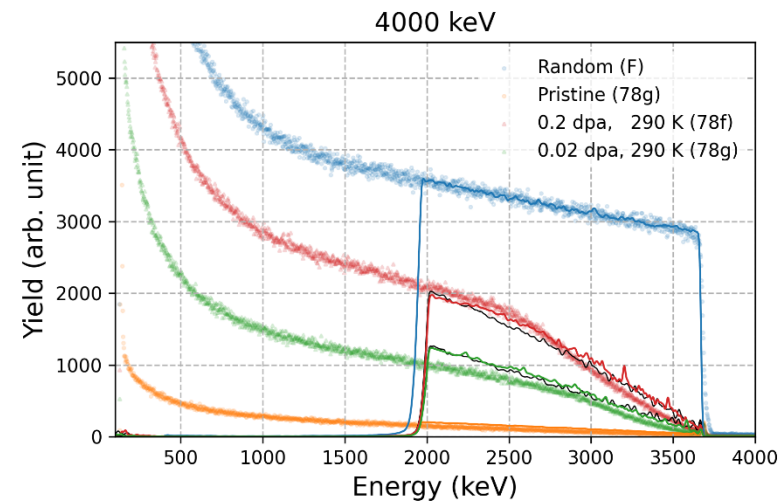
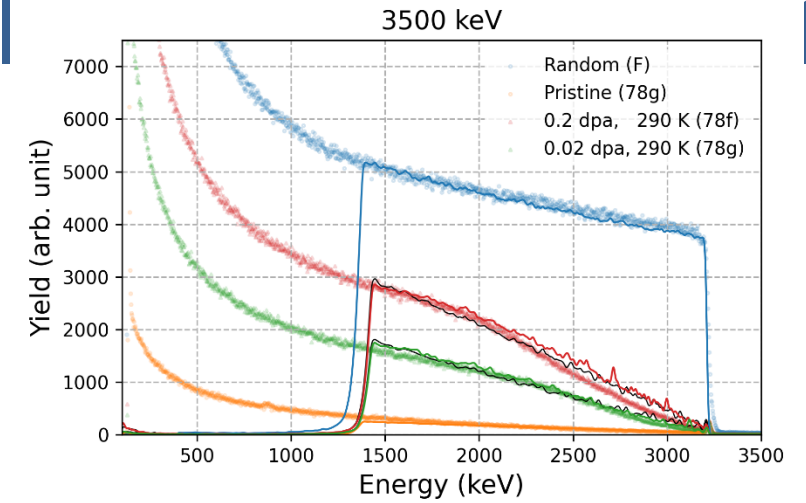
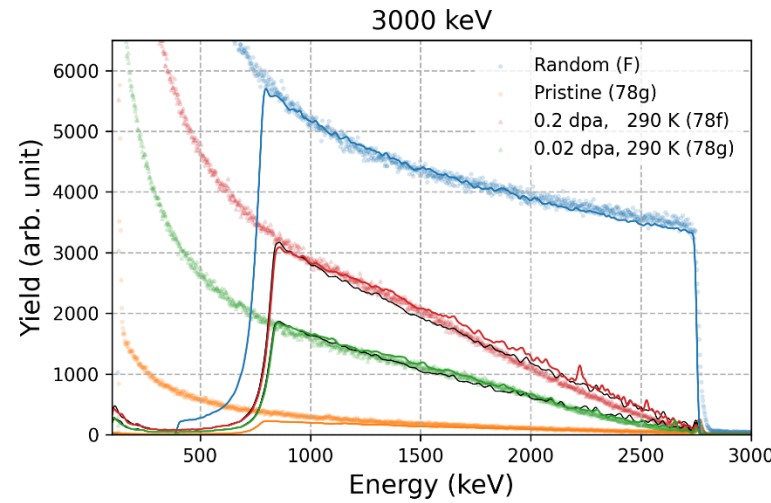
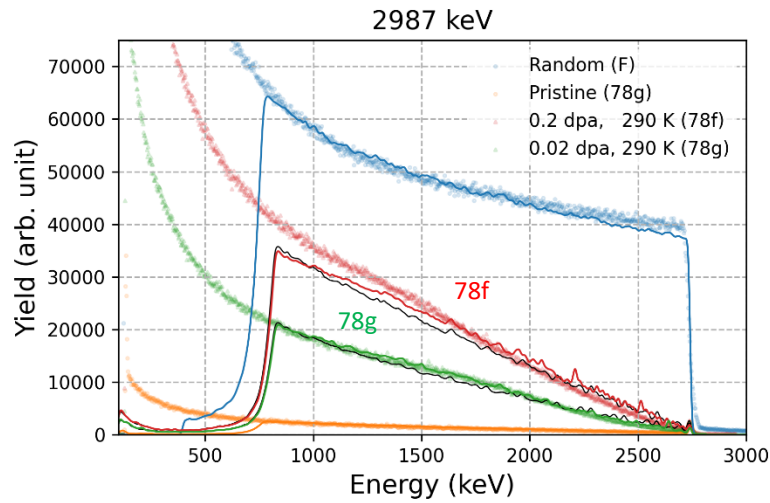
➤ The SRIM dpa depth profile is transformed to a collision cascade number profile.

- Then MD boxes (70) with the corresponding cascade number are stacked along the direction of depth.



➤ Good agreement between simulation and experiment results (especially sample 78g)

C-RBS spectra as a function of energy (MD calculations and fits)



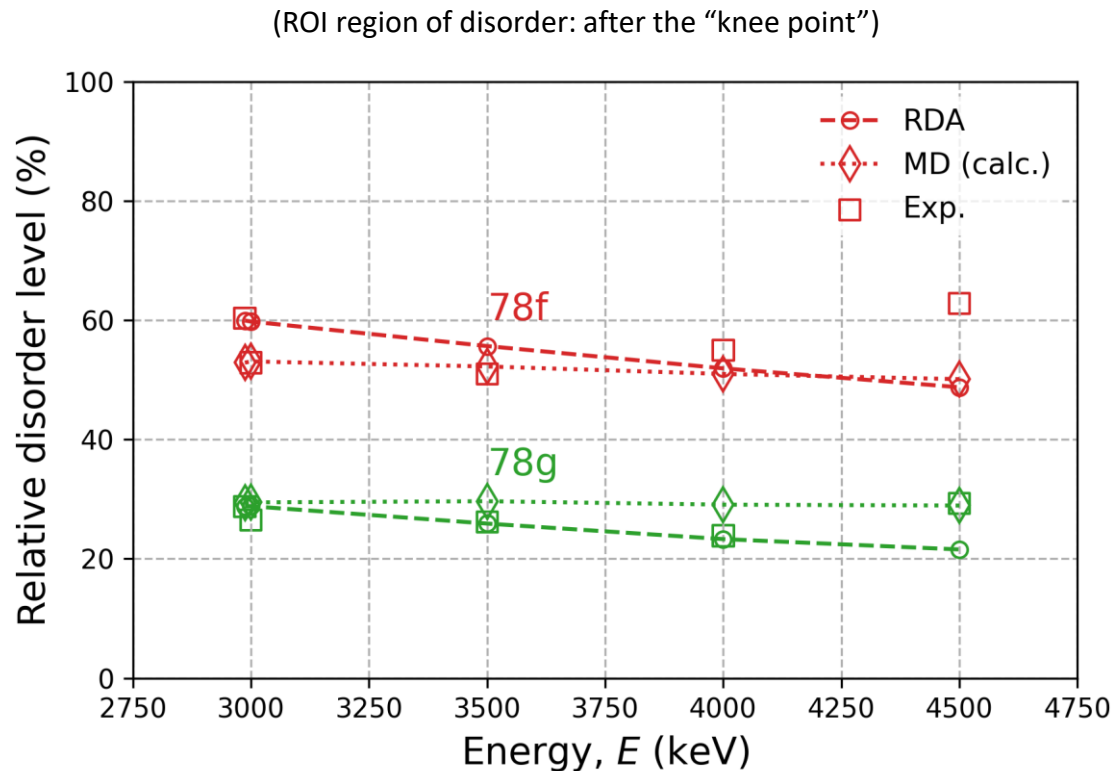
(For MD fits, red and green regions of sample 78f for the RBS/C spectra of sample 78f and 78g, respectively)

- Dislocations in MD cells: mainly dislocation loops

3 MeV → 4.5 MeV

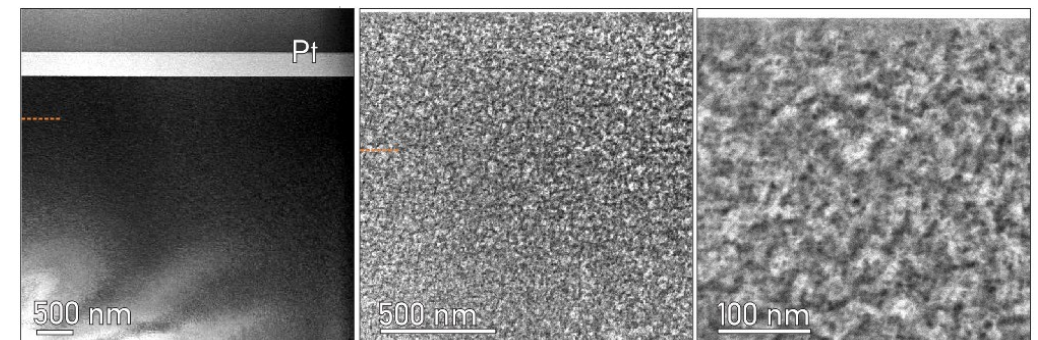
- Sample 78f: simulation spectra becomes smaller compared to experiments with a higher energy
- Sample 78g: simulation spectra follows experiments well

C-RBS signals as a function of energy



- Sample 78f (exp): increases with E
- Sample 78g (exp): roughly constant
- RDA: decreases with E
- MD (dislocation loops): almost constant

- Sample 78f (exp): neither RDAs nor dislocation loops in the MD cells (should be larger loops or lines as observed in previous TEM experiments)
- Sample 78g (exp): Dislocation loops in the MD cells
TEM images of 78g: dislocation loops were observed





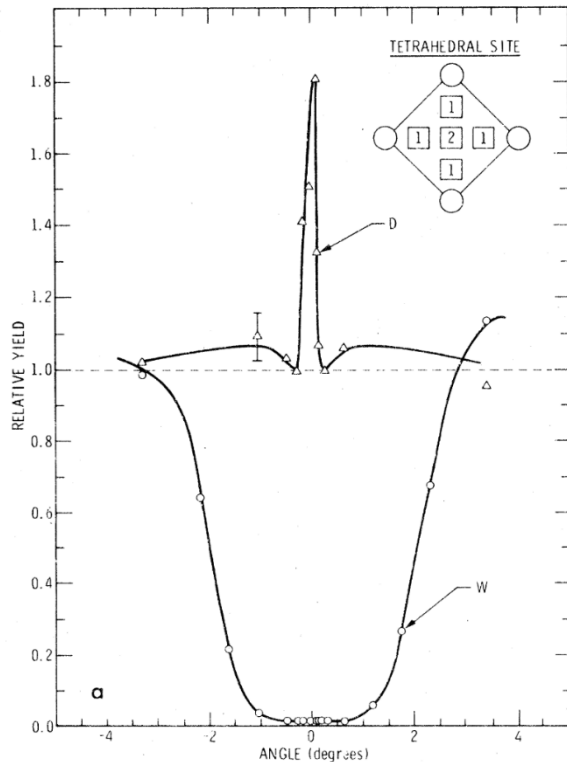
- Task 1.1 Incorporation of the goniometer in the INSIBA experimental station – JSI.
 - D2.1 (Task 1.1) Commissioning of the goniometer with cooling and heating capabilities. (M1)
- Task 1.2 Detection system for ion beam methods
 - D2.2 (Task 1.2) Purchase of the PSD and acquisition system. (M2)
- Task 2.1 Production of samples with dominant defects in the material – MPG and JSI.
 - Second batch with well-defined displacement damage.
- Task 2.2 Characterization of defects –UHEL, JSI, MPG.
 - D2.3 (Task 2.2) Microstructure data on samples with dominant defect type, first C-RBS spectra. (M4)
- Task 2.3 Simulation and interpretation of C-RBS spectra - UHEL, CEA, JSI.
 - D2.4 (Task 2.3) Incorporation of defect structures into RBSADEC. (M5)
- Task 3.1 Characterization of defects by D retention studies and MRE modelling - JSI, MPG, CEA, UHEL.
 - D2.5 (Task 3.1) Determine the de-trapping energies of D in defects and correlate with the defect characterization techniques. (M7)
- Task 3.3 – Modelling of deuterium position in lattice/defect and identification of D position - UHEL, CEA, JSI.
 - D2.6 (Task 3.3) DFT calculations for D positions in defects, code development for C-NRA.

Development of C-NRA simulation and detection of D by RBSADEC code



Experiments in literature

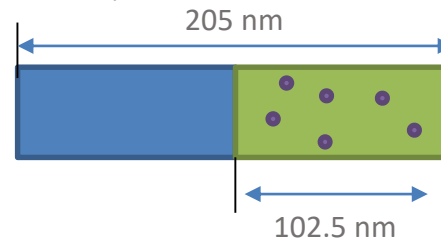
- Incident ions: 750 keV ^3He ions
- Nuclear reaction: $\text{D} (^3\text{He}, \text{p}) ^4\text{He}$
- Detector angle: 135 degree
- Angular scan: around $\langle 100 \rangle$ axis of W
- D location: tetrahedral sites



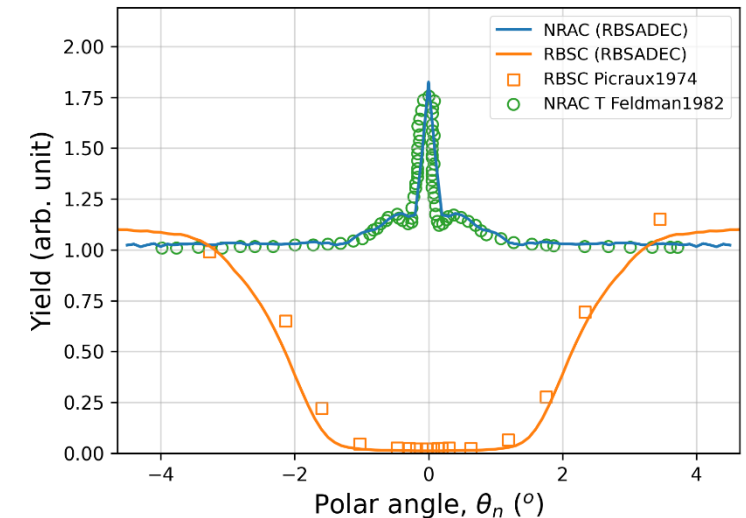
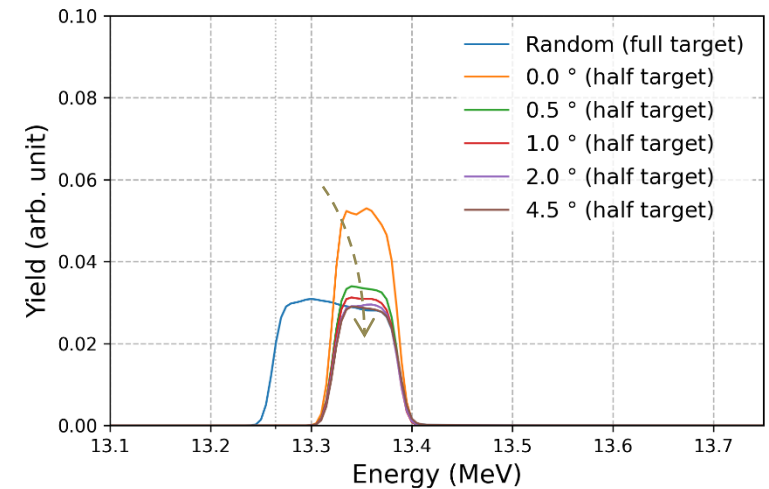
(S. Picraux, Phys. Rev. Lett., 33, 1974)

Incorporation of C-NRA into RBSADEC

- RBS/C: a pristine W target
- NRA/C:



- The first half is pristine: to establish a stable distribution of incident ions
- The second half : 0.1 % of D at tetrahedral sites
- Comparison of C-NRA simulation with literature**
(L. Feldman et al, Materials Analysis by Ion Channeling, 1982)
- Different simulation result compared to experiment – not unexpected

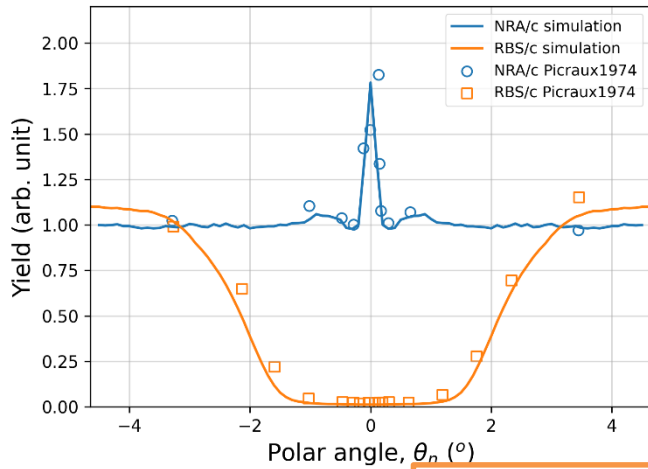


C-NRA simulations, fit of experimental spectra



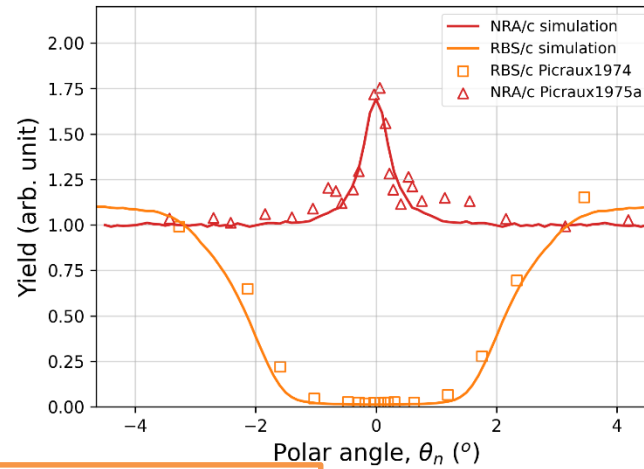
$3 \times 10^{15} \text{ cm}^{-2}$ 30 keV D on W

(S. Picraux, Phys. Rev. Lett., 33, 1974)

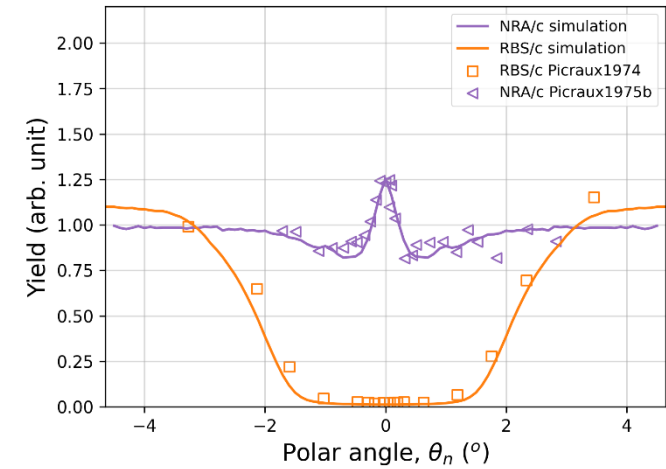


$1 \times 10^{15} \text{ cm}^{-2}$ 15 keV D on W

(S. Picraux, Ion Implantation in Semiconductors, 1975, 355-360)

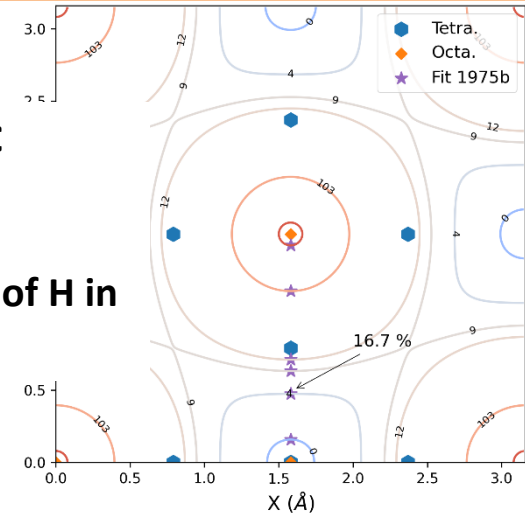
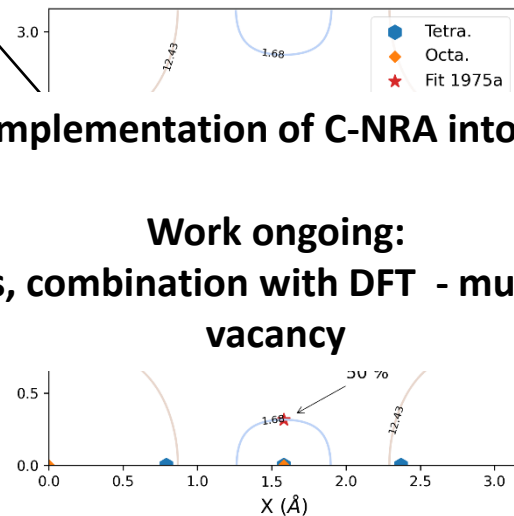
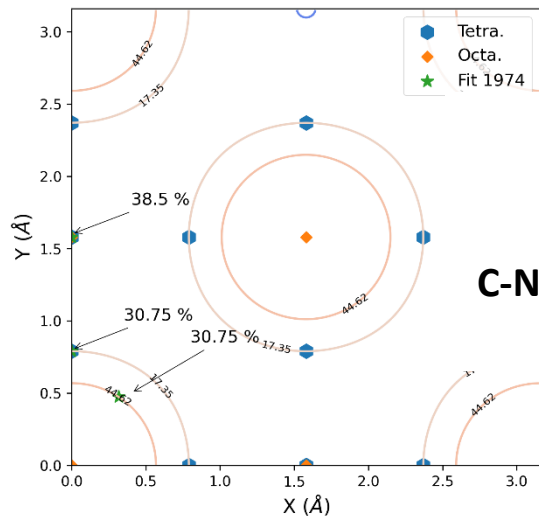


$1 \times 10^{15} \text{ cm}^{-2}$ 15 keV D on W
 $3.7 \times 10^{16} \text{ cm}^{-2}$ 750 keV ^3He on W



Close to tetrahedral sites

Some close to octahedral sites



Successful implementation of C-NRA into the RBSADEC

Work ongoing:
 C-NRA simulations, combination with DFT - multi occupancy of H in vacancy

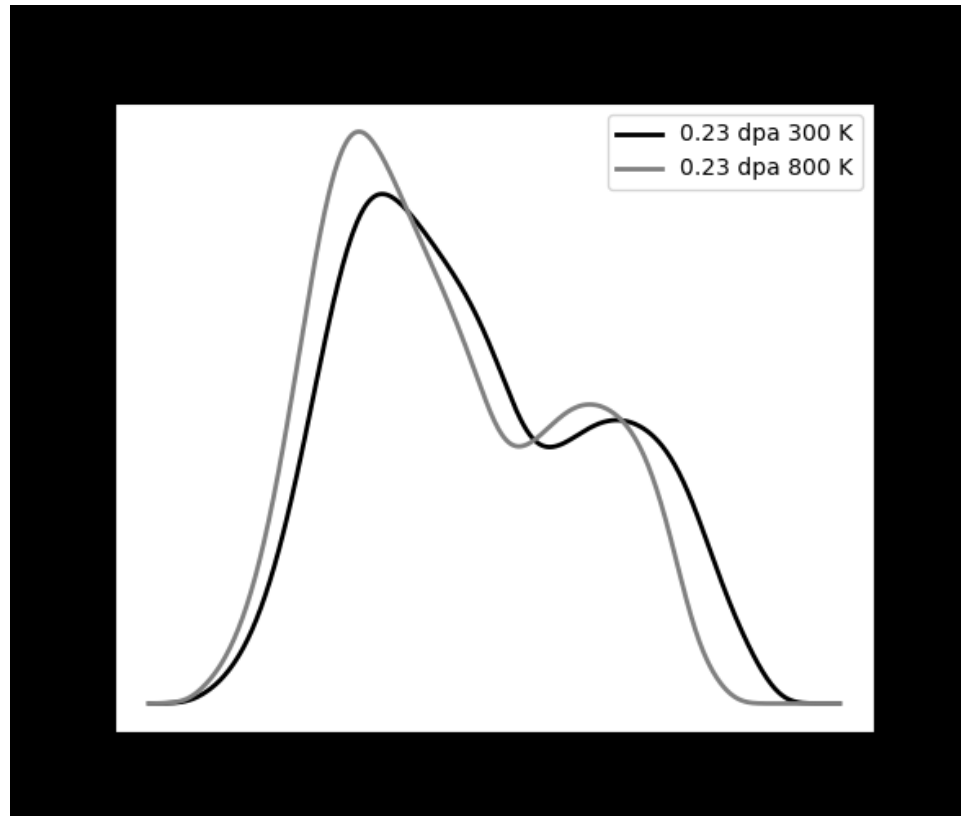


- Task 1.1 Incorporation of the goniometer in the INSIBA experimental station – JSI.
 - D2.1 (Task 1.1) Commissioning of the goniometer with cooling and heating capabilities. (M1)
- Task 1.2 Detection system for ion beam methods
 - D2.2 (Task 1.2) Purchase of the PSD and acquisition system. (M2)
- Task 2.1 Production of samples with dominant defects in the material – MPG and JSI.
 - Second batch with well-defined displacement damage.
- Task 2.2 Characterization of defects –UHEL, JSI, MPG.
 - D2.3 (Task 2.2) Microstructure data on samples with dominant defect type, first C-RBS spectra. (M4)
- Task 2.3 Simulation and interpretation of C-RBS spectra - UHEL, CEA, JSI.
 - D2.4 (Task 2.3) Incorporation of defect structures into RBSADEC. (M5)
- Task 3.1 Characterization of defects by D retention studies and MRE modelling - JSI, MPG, CEA, UHEL.
 - D2.5 (Task 3.1) Determine the de-trapping energies of D in defects and correlate with the defect characterization techniques. (M7)
- Task 3.3 – Modelling of deuterium position in lattice/defect and identification of D position - UHEL, CEA, JSI.
 - D2.6 (Task 3.3) DFT calculations for D positions in defects, code development for C-NRA.

Macroscopic Rate Equation (MRE) modelling with MHIMS code: Simulated TDS spectra

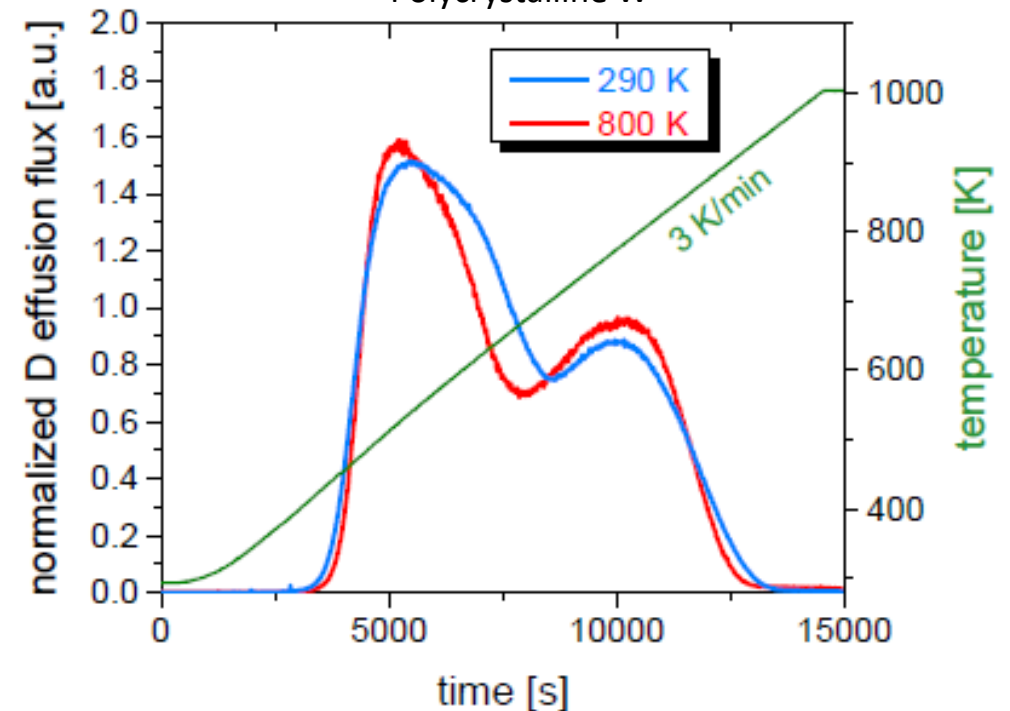
- ❑ From fitting the D depth profiles and TDS spectra we obtain the information of defect concentration and de-trapping energies for different damaging scenarios
- ❑ Input for RBSADEC code / Compare to MD simulations
 - ❑ Comparison of simulated and experimental TDS spectra between damaging at 300 K and damaging at 800 K

$$\frac{\varphi_{\text{des}}(t)}{\int \varphi_{\text{des}}(t) dt}$$



different dpa ongoing

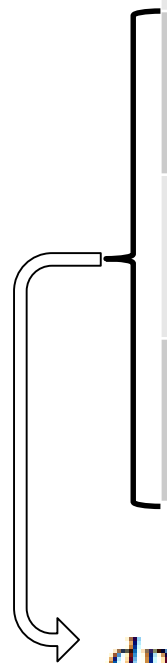
0.23 dpa, D decoration 370 K
Polycrystalline W



Macroscopic Rate Equation (MRE) modelling: Trapping sites in the simulations

D trapping energies and defect concentrations from M. Pečovnik's papers (NF 60 (2020) 036024 and JNM 550 (2021))

Defect type	Detrapping energies	Trap concentration (at.fr)
Intrinsic trap I	0.85 eV	2×10^{-5}
Intrinsic trap II	1.00 eV	2×10^{-5}
Type I: monovacancies	5 levels: 1.08 eV – 1.46 eV	0.220×10^{-2} at 300K ($\eta = 1.5 \times 10^9$) 0.070×10^{-2} at 800K ($\eta = 0.5 \times 10^9$)
Type II: Medium size vacancy clusters ($\sim V_6$)	2 levels 1.68 – 1.86 eV	0.290×10^{-2} at 300 K ($\eta = 1.5 \times 10^9$) 0.110×10^{-2} at 800 K ($\eta = 0.5 \times 10^9$)
Type III: Big vacancy clusters (\Leftrightarrow Surfaces)	2.05 eV	0.050×10^{-2} at 300 K ($\eta = 1.5 \times 10^9$) 0.005×10^{-2} at 800 K ($\eta = 0.5 \times 10^9$)



From SRIM

$$\frac{dn_i(x, t)}{dt} = \frac{\Gamma \eta \Theta(x)}{\rho} \left[1 - \frac{n_i(x, t)}{n_{i, \max}} \right]$$



- **WP 4 management** - four zoom meetings organized with the team members, details and presentations available on Indico, links to indico sites on Wiki page https://wiki.euro-fusion.org/wiki/Project_No4
- February 2022
- June 2022
- September 2022
- December 2022

- **Conferences:**
 - Two contributions at PFMC, May 2023
 - Two contributions at ICFRM, October 2023

- **Papers:**
 - 1 manuscripts in preparation
 - Accepted in December 2022: Jin et al. Effect of lattice voids on Rutherford backscattering dechanneling in tungsten, J. Phys. D: Appl. Phys. 56 (2023) 065303, <https://doi.org/10.1088/1361-6463/acad12>

Tasks and deliverables in 2022



- Task 1.1 Incorporation of the goniometer in the INSIBA experimental station – JSI.

- **D2.1 (Task 1.1)** Commissioning of the goniometer with cooling and heating capabilities. (M1)

- Task 1.2 Detection system for ion beam methods

- **D2.2 (Task 1.2)** Purchase of the PSD and acquisition system. (M2)

- Task 2.1 Production of samples with dominant defects in the material – MPG and JSI.

- Second batch with well-defined displacement damage.

- Task 2.2 Characterization of defects –UHEL, JSI, MPG.

- **D2.3 (Task 2.2)** Microstructure data on samples with dominant defect type, first C-RBS spectra. (M4)

- Task 2.3 Simulation and interpretation of C-RBS spectra - UHEL, CEA, JSI.

- **D2.4 (Task 2.3)** Incorporation of defect structures into RBSADEC. (M5)

- Task 3.1 Characterization of defects by D retention studies and MRE modelling - JSI, MPG, CEA, UHEL.

- **D2.5 (Task 3.1)** Determine the de-trapping energies of D in defects and correlate with the defect characterization techniques. (M7)

- Task 3.3 – Modelling of deuterium position in lattice/defect and identification of D position - UHEL, CEA, JSI.

- **D2.6 (Task 3.3)** DFT calculations for D positions in defects, code development for C-NRA.



On schedule



Delayed

Tasks and objectives in 2023



- Task 1.1 Incorporation of the goniometer in the INSIBA experimental station – JSI.
- Task 1.2 Detection system for ion beam methods
 - ❖ **O3.1 (Task 1.1) C-RBS spectra obtained with new channeling set-up. (D1)**
- Task 2.1 Production of samples with dominant defects in the material – MPG and JSI.
- Task 2.2 Characterization of defects –UHEL, JSI, MPG.
- Task 2.3 Simulation and interpretation of C-RBS spectra - UHEL, CEA, JSI.
 - ❖ **O3.2 (Task 2.2, 2.3, 3.1) Defect identification by C-RBS and correlation to TEM and PAS measurements – report. (D2)**
- Task 2.4 In-situ C-RBS and sample heating – JSI
 - ❖ **O3.3 (Task 2.4) In-situ sample heating in INSIBA-C. (M6)**
- Task 3.1 Characterization of defects by D retention studies and MRE modelling - JSI, MPG, CEA, UHEL.
- Task 3.2 Development of C-NRA method - JSI, UHEL, MPG.
 - ❖ **O3.4 (Task 3.1 and Task 3.2) Detection of deuterium by C-NRA method. (M8)**
- Task 3.3 – Modelling of deuterium position in lattice/defect and identification of D position - UHEL, CEA, JSI.
 - ❖ **O3.5 (Task 3.3) Incorporation of C-NRA in RBSADEC. (M9)**

Thank you for your attention